



ALMA MATER STUDIORUM
UNIVERSITÀ DI BOLOGNA

ARCHIVIO ISTITUZIONALE DELLA RICERCA

Alma Mater Studiorum Università di Bologna Archivio istituzionale della ricerca

Ecological regime shift preserved in the Anthropocene stratigraphic record

This is the final peer-reviewed author's accepted manuscript (postprint) of the following publication:

Published Version:

Ecological regime shift preserved in the Anthropocene stratigraphic record / Tomasovych A.; Albano P.G.; Fuksi T.; Gallmetzer I.; Haselmair A.; Kowalewski M.; Nawrot R.; Nerlovic V.; Scarponi D.; Zuschin M.. - In: PROCEEDINGS - ROYAL SOCIETY. BIOLOGICAL SCIENCES. - ISSN 1471-2954. - STAMPA. - 287:1929(2020), pp. 20200695.1-20200695.9. [10.1098/rspb.2020.0695]

Availability:

This version is available at: <https://hdl.handle.net/11585/766621> since: 2021-02-25

Published:

DOI: <http://doi.org/10.1098/rspb.2020.0695>

Terms of use:

Some rights reserved. The terms and conditions for the reuse of this version of the manuscript are specified in the publishing policy. For all terms of use and more information see the publisher's website.

This item was downloaded from IRIS Università di Bologna (<https://cris.unibo.it/>).
When citing, please refer to the published version.

(Article begins on next page)

This is the final peer-reviewed accepted manuscript of:

Tomasovych A.; Albano P.G.; Fuksi T.; Gallmetzer I.; Haselmair A.; Kowalewski M.; Nawrot R.; Nerlovic V.; Scarponi D.; Zuschin M.: *Ecological regime shift preserved in the Anthropocene stratigraphic record*

PROCEEDINGS - ROYAL SOCIETY. BIOLOGICAL SCIENCES VOL. 287 ISSN 1471-2954

DOI: 10.1098/rspb.2020.0695

The final published version is available online at:

<https://dx.doi.org/10.1098/rspb.2020.0695>

Terms of use:

Some rights reserved. The terms and conditions for the reuse of this version of the manuscript are specified in the publishing policy. For all terms of use and more information see the publisher's website.

This item was downloaded from IRIS Università di Bologna (<https://cris.unibo.it/>)

When citing, please refer to the published version.

PROCEEDINGS OF THE ROYAL SOCIETY B

BIOLOGICAL SCIENCES

Ecological regime shift preserved in the Anthropocene stratigraphic record

Journal:	<i>Proceedings B</i>
Manuscript ID	RSPB-2020-0695
Article Type:	Research
Date Submitted by the Author:	27-Mar-2020
Complete List of Authors:	Tomasovych, Adam; Slovak Academy of Sciences, Earth Science Institute Albano, Paolo; University of Vienna, Department of Palaeontology Fuksi, Tomas; Slovak Academy of Sciences, Earth Science Institute Gallmetzer, Ivo; University of Vienna, Department of Palaeontology Haselmair, Alexandra; University of Vienna, Department of Palaeontology Kowalewski, Michal; University of Florida, Florida Museum of Natural History Nawrot, Rafał; University of Vienna, Department of Palaeontology Nerlovic, Vedrana; University of Split, Department of Marine Sciences Scarponi, Daniele; University of Bologna, Dipartimento di Scienze Biologiche, Geologiche e Ambientali Zuschin, Martin; University of Vienna, Department of Palaeontology
Subject:	Palaeontology < BIOLOGY, Ecology < BIOLOGY
Keywords:	conservation paleobiology, stratigraphic paleobiology, time averaging, regime shift, stasis, Adriatic Sea
Proceedings B category:	Palaeobiology

SCHOLARONE™
Manuscripts

Author-supplied statements

Relevant information will appear here if provided.

Ethics

Does your article include research that required ethical approval or permits?:

This article does not present research with ethical considerations

Statement (if applicable):

CUST_IF_YES_ETHICS :No data available.

Data

It is a condition of publication that data, code and materials supporting your paper are made publicly available. Does your paper present new data?:

Yes

Statement (if applicable):

All size and compositional data are attached in an excel file in the Supplement, plus source codes in R language

Conflict of interest

I/We declare we have no competing interests

Statement (if applicable):

CUST_STATE_CONFLICT :No data available.

Authors' contributions

This paper has multiple authors and our individual contributions were as below

Statement (if applicable):

A.T. and M.Z. designed the research, P.A., T.F., I.G., A.H., M.K., R.N., V.N. and D.S. collected the data, A.T. compiled and analyzed the data, and all authors discussed the results and contributed to the writing of the manuscript.

1 Title: Ecological regime shift preserved in the Anthropocene stratigraphic record

2

3 Running Head: Regime shift in the stratigraphic record

4

5 Authors: Adam Tomašových^{1,2}, Paolo G. Albano², Tomáš Fuksi¹, Ivo Gallmetzer², Alex
6 Haselmair², Michał Kowalewski³, Rafał Nawrot², Vedrana Nerlović⁴, Daniele Scarponi⁵,
7 Martin Zuschin²

8

9 Affiliations: ¹Earth Science Institute, Slovak Academy of Sciences, Dúbravská cesta 9, 84005
10 Bratislava, Slovakia

11 ²University of Vienna, Department of Palaeontology, Althanstrasse 14, 1090 Vienna

12 ³Florida Museum of Natural History, University of Florida, 1659 Museum Road, Gainesville,
13 FL 32611, USA

14 ⁴Department of Marine Studies, University of Split, Ruđera Boškovića 37, 21000 Split,
15 Croatia

16 ⁵Department of Biological, Geological and Environmental Sciences, University of Bologna,
17 Piazza di Porta San Donato 1, I-40126 Bologna, Italy

18

19

20 Corresponding author: Adam Tomašových, Earth Science, Slovak Academy of Sciences,
21 Dúbravská cesta 9, 84005 Bratislava, Slovakia. Tel: 00421-904-852145, Email:
22 geoltoma@savba.sk

23

24 Keywords: conservation paleobiology, stratigraphic paleobiology, stasis, regime shift, time

25 averaging, northern Adriatic Sea

26 **SUMMARY**

27 Paleocological data are unique historical archives that extend back far beyond the last several
28 decades of ecological observations. However, the fossil record of continental shelves has been
29 perceived as too coarse and incomplete to detect processes occurring at decadal scales
30 relevant to ecology and conservation. Here we show that the youngest (Anthropocene) fossil
31 record on a continental shelf of the Adriatic Sea provides decadal-scale temporal resolution
32 that is adequate for documenting an abrupt ecological shift affecting benthic communities
33 during the 20th century. The magnitude and the duration of the 20th century shift in body size
34 of a dominant bivalve species (*Corbula gibba*) is unprecedented given that this species was
35 consistently small throughout the Holocene in the whole northern Adriatic Sea. The size shift
36 coincided with compositional change of the benthic community, with the median per-
37 assemblage abundance of *C. gibba* increasing from ~25% to ~70% in the late 20th century,
38 and occurred at sites that experienced at least one hypoxic event per decade in the 20th
39 century. This regime shift, which coincided with mass mortality of competitors and predators
40 associated with higher frequency of seasonal hypoxic events, may reflect ecological release.
41 The observed body size shift is coupled with a decline in the depth and rate of bioturbational
42 mixing. This decline in burrowing benthic organisms resulted in the improved stratigraphic
43 resolution of fossil assemblages, making it possible to detect sub-centennial ecological
44 changes in the stratigraphic record on continental shelves.

45

46 **Significance statement**

47 The stratigraphic records of deep-time ecosystem perturbations are not equivalent to
48 chronological records of Anthropocene ecological collapses because these two types of
49 archives differ in stratigraphic completeness and time averaging. Although conservation
50 paleobiology approaches identify past baselines and detect differences between the Holocene

51 and present-day communities, it remains unclear if Holocene-Anthropocene stratigraphic
52 records can inform us about rates of ecological change. We show that the 20th century
53 stratigraphic record of molluscan assemblages in cores in the Adriatic Sea uniquely detects an
54 abrupt, decadal-scale regime shift in size structure and species composition of molluscan
55 assemblages that has no precedents in the Holocene record. This decadal-scale resolution was
56 made possible by intensification of hypoxia that not only led to a competitive and predatory
57 release but also reduced bioturbation and thus enhanced temporal resolution of the
58 stratigraphic record. We highlight a dichotomy in the resolution of the fossil record between
59 background regimes with low incidence of major ecosystem perturbations with highly time-
60 averaged fossil assemblages and disturbance or extinction regimes such as Anthropocene
61 when limited bioturbation suppresses time averaging.

62

64 **1. Introduction**

65 Although high-resolution time series based on monitoring of living assemblages can directly
66 detect the dynamics of marine ecosystem responses to stressors (1-5), their duration is
67 typically decadal (6-7). Therefore, they might not detect former baseline states or discriminate
68 short-term fluctuations from sustained regime shifts. In contrast, surface and subsurface
69 stratigraphic records that capture longer durations led to unique discoveries of ecosystem
70 shifts driven by pollution, eutrophication or overfishing that occurred over the past centuries
71 or millennia (8-12). These shifts can be comparable in magnitude to ecological crises that
72 occurred during the mass extinctions when deoxygenation and warming also significantly
73 contributed to the demise of ecosystems (13-15). However, determining whether the
74 ecological changes were gradual or abrupt on the basis of the stratigraphic record is hindered
75 by hiatuses (induced by erosion and non-deposition) and by time averaging (mixing of non-
76 contemporaneous generations) (16-17), unless bioturbation is limited and erosion is rare or
77 episodic as in lacustrine or anoxic environments (18-20). As a result, benthic fossil
78 assemblages from continental shelves – settings that provide the bulk of the deep-time
79 paleontological data on ecological dynamics – are incomplete and temporally mixed over 10^3 -
80 10^4 -year time scales (21-22). On one hand, both the hiatuses and the time averaging of
81 bioturbated sediments depress the magnitude of ecological change *over a given timespan* (23-
82 25). On the other hand, hiatuses can generate apparently abrupt shifts in the magnitude of
83 ecological change *over a given stratigraphic distance* even in the absence of truly abrupt
84 regime shifts, confounding assessments of ecological turnover on the basis of stratigraphic
85 records (24-26).

86 The Holocene cores recording anthropogenic impacts provide a unique testing
87 opportunity to assess whether the response of marine ecosystems exposed to disturbance can
88 be resolved from stratigraphic records. Here, absolute dating of shells embedded in sediment

89 cores allows us to directly compare *chronological* (i.e., ages of fossils in time series do not
90 depend on their stratigraphic position, here partitioned into 5-year age cohorts) and
91 *stratigraphic* records (i.e., ages of fossils refer to the mean age of a sedimentary layer in
92 which they are embedded). We test whether the responses of benthic communities to
93 eutrophication and hypoxic events that intensified in the Adriatic Sea (figure 1A) during the
94 late 20th century left high-resolution signatures in the Anthropocene stratigraphic record
95 (informally denoting here the 20th and 21st centuries) (1) by assessing chronologic and
96 stratigraphic changes in mean and maximum body size of an opportunistic and hypoxia-
97 tolerant bivalve (*Corbula gibba*) in sediment cores and (2) by comparing molluscan species
98 composition between Holocene and Anthropocene assemblages. We suggest that bioturbated
99 sediment cores can generate high-resolution windows into ecological dynamics induced by
100 disturbances such as oxygen depletion that subsequently limit sediment mixing.

101 We focus on body size because this attribute tracks ecosystem changes during natural
102 (27) and anthropogenic disturbances of ecosystems (28-29) and also predicts present-day
103 extinction threat of marine molluscs (30). We combine body size estimates based on valve
104 length measurements of 20,774 specimens of *C. gibba* collected with cores split into ~5-10
105 cm-thick increments and 14 surface death assemblages with formerly-published estimates of
106 time averaging based on radiocarbon-calibrated amino acid racemization (figure 2, see
107 electronic supplementary material, ESM). First, we identify the number and timing of abrupt
108 shifts in the mean and the 95th percentile log-length in chronological and stratigraphic records
109 with the threshold regression (31). Second, we test whether models that allow for abrupt shifts
110 in size have higher support than models with stasis or trends (32) and assess their sensitivity
111 to time averaging. Third, we assess whether these shifts covary with independent estimates of
112 changes in bottom-water oxygen concentrations and whether they are associated with
113 compositional changes in molluscan communities.

114

115 **2. Methods**

116 **(a) Sediment cores, dating, and time averaging.** Death assemblages of *Corbula gibba* were
117 collected in Holocene cores and with Van Veen grabs in the northern Adriatic Sea. First, 1.5
118 m-long cores were collected at eight sites at water depths between 10 and 44 m (two sites at
119 Po prodelta, two sites at Isonzo prodelta, two sites off Piran, and one site at Venice and
120 Brijuni). Second, one 26 m-long Holocene section of S10 core was collected at the Po Plain
121 (33). Third, Van Veen grabs (~upper 10 cm) were collected at 14 sites at Po prodelta (2 sites),
122 in the Gulf of Venice (2 sites), off Rovinj (2 sites), and in the Bay of Panzano (Isonzo
123 prodelta) in the northern Gulf of Trieste (8 sites) (figure S1). Estimates of increment ages,
124 sedimentation rates, and time averaging of all cores based on ages (AAR calibrated by ^{14}C) of
125 four targeted molluscan species were published in our previous studies (34-40). Time
126 averaging corresponds to an inter-quartile age range in years (IQR) in ~10-30 cm-thick units
127 on the basis of AAR calibrated by ^{14}C in four molluscan species (34-40). Net sedimentation
128 rate was ~0.3 cm/y during the transgressive phase (TST) and 1-2 cm/y during the highstand
129 phase (HST) at Po prodelta, 0.2-0.4 cm/y during the HST phase at Isonzo prodelta, and ~0.01
130 cm/y during the TST and HST phases off Istria and in the Gulf of Venice (36-40). The
131 uppermost HST increments (corresponding to 20th century sediments) do not show any signs
132 of increased or decreased sedimentation rate (36). The differences in net sedimentation rates
133 translate to differences in IQR. First, highly time-averaged assemblages (IQR = ~1,000-2,000
134 years) occur in TST (S10, Venice, Piran, Brijuni) and HST increments (Venice, Piran,
135 Brijuni), including mixtures of highstand and Anthropocene shells in topcore and surface
136 assemblages at Rovinj, Venice, Piran, and Brijuni. Second, weakly time-averaged
137 assemblages (IQR = ~10-200 years) occur in HST increments and Anthropocene increments
138 at Po and Isonzo prodeltas. The cores with weakly time-averaged assemblages show a

139 significant upcore decline in IQR in the 20th century sediments at Po (from decadal to yearly
140 IQR) and Isonzo prodeltas (from centennial to decadal IQR, 36). This stratigraphic upcore
141 decline in IQR is driven by a decrease in the bioturbation depth and rate rather than by an
142 increase in sedimentation rate (36).

143

144 **(b) Size data.** We measured shell size with the length of right valves in 20,774 specimens of
145 *C. gibba*. *Chronological* analyses in body size are based on lengths of specimens from two Po
146 cores that were directly dated (36) and were partitioned into 5-year age cohorts (table S1-S2,
147 252 dated specimens at Po 3 and 243 dated specimens at Po 4, sample sizes of cohorts that
148 lived in the 19th and 20th century in other cores are low). *Stratigraphic* analyses of size
149 distributions are performed (1) at the scale of 5-10 cm-thick increments and (2) by pooling
150 these increments to 10-30 cm-thick units characterized by homogeneous sedimentologic
151 composition (72 samples in total) and at two spatial scales, including (1) pooling closely-
152 located sites to three localities (Po, Isonzo, Piran), and (2) at the scale of eight individual sites
153 (table S1, S3-S4). Size data are available in the electronic supplementary material.

154

155 **(c) Multivariate size analyses.** We assess whether size structure did undergo a shift in the
156 20th century to a new state, using principal coordinate analysis, with the Frechet distances
157 between 10-30 cm-thick increments, based on proportional abundances of 1 mm cohorts and
158 (figure S2A-B). The multivariate analyses are thus based on 72 samples (in analyses based on
159 all shells based on 20,774 specimens) and 66 samples (in analyses based on shells with
160 periostracum based on 13,985 specimens). They are assigned to four stratigraphic units,
161 including (1) TST (between 10-7 kyr ago), (2) HST (here, referring to increments deposited
162 prior to the late 20th century), (3) topcore samples with a strongly time-averaged mixture of
163 the HST and the 20th century sediments deposited under <0.01 cm/y (HST-Anthropocene),

164 and (4) the topcore samples at Po and Isonzo prodeltas deposited under >0.2 cm/y and
165 corresponding to the late 20th century (Anthropocene). We use analogue matching analyses to
166 assess whether Anthropocene assemblages extend beyond the variation defined by all
167 Holocene (TST and HST) assemblages in terms of Frechet distances between the Holocene
168 centroid and individual Anthropocene assemblages (41-44) and evaluate differences in size
169 structure between four stratigraphic units with permutational multivariate analysis of variance
170 (PERMANOVA, 45). To untangle these cohorts, we scored all shells in Van Veen grab
171 samples on the basis of periostracum preservation. Periostracum is usually not preserved on
172 shells older than 19th-20th century (figure S3).

173
174 **(d) Detection of regime shifts and sensitivity to time averaging.** We compare chronological
175 and stratigraphic records in (i) the mean and (ii) the 95% percentile log-length. The mean
176 length captures the central tendency across the whole size range of death assemblages,
177 including juvenile specimens, whereas the 95% percentile length is informative about the size
178 structure of adult individuals. We use three approaches to detect the regime shifts (i.e., a
179 large, abrupt, and persistent shift in ecosystem structure), here approximated by shift in the
180 size structure of one of the most abundant molluscan species). First, a threshold regression
181 identifies abrupt shifts and their location in chronological or stratigraphic time series. We use
182 an F statistic that evaluates whether the model with one shift explains significantly more than
183 the model with just an intercept (31) and the adjusted R^2 to compare the threshold model with
184 a simple linear model. Second, we fit chronological or stratigraphic time series of size to
185 likelihood models of the unbiased random walk, stasis, and directional trends (32, 46-47). In
186 total, the likelihood models discriminate among four modes (stasis, strict stasis, random walk,
187 and directional models) and allow for one abrupt shift between them (nine models in total, we
188 set the minimum segment length to 7 samples). The stasis model is considered as

189 uncorrelated, normally-distributed variation in size (either in the mean or in the 95th
190 percentile log-length), with temporal variance ω around a stable long-term mean θ (48). Size
191 is expected to converge immediately to θ from any precursor (ancestral) value. The variance
192 ω is zero under the so-called strict stasis. Directional shift in body size models a size change
193 for each time step on the basis of a normal distribution of size changes, with mean size change
194 μ_s and a variance of size changes δ_s^2 . A random walk is a special case of the directional model
195 in which μ_s is equal to zero and the distribution of size changes is also normal, with variance
196 also equal to δ_s^2 . The punctuation model refers to one abrupt shift separated by two segments
197 of stasis with θ_1 and θ_2 and a single ω , and is thus conceptually most comparable to the
198 definition of the regime shift. We estimate the number and timing of shifts with threshold
199 regression (figure S4-S6) and the support for nine models in (1) whole cores and (2) core
200 subsets with HST and Anthropocene increments for both chronologic and stratigraphic series
201 (table S3-S4). Third, we correlate the model support and ω with time averaging (IQR) for (1)
202 the HST core subsets and (2) the core subsets with HST and Anthropocene increments.

203

204 **(e) Covariates of size shifts.** We assess the response of the mean and 95th percentile log-
205 length to a hypothesized driver - yearly frequency of seasonal hypoxia (dissolved oxygen
206 concentrations < 2 ml/L) on the basis of instrumental measurements performed between 1970-
207 2010 - with the threshold regression and generalized additive models. Second, we compare
208 the taxonomic composition of molluscan assemblages with TST and HST assemblages on one
209 hand (deposited prior to the 20th century or during the earliest 20th century, 95 assemblages
210 from the same cores used in analyses of shell size) with 54 Anthropocene death assemblages
211 (late 20th century) and 223 Anthropocene living assemblages collected since 1980s on the
212 other hand (Van Veen grab samples compiled from published sources). The Anthropocene
213 data are based on multiple studies by various authors of soft-bottom habitats in the Po

214 prodelta and in the Gulf of Trieste between 10-30 m water depth (with sample size exceeding
215 30) and are thus standardized to genus level. The compositions of Anthropocene living
216 assemblages are not affected by mixing and thus help constraining the compositional state of
217 the latest 20th century communities. Compositional differences are analyzed with principal
218 coordinate analysis, PERMANOVA (Bray-Curtis distances based on square-root transformed
219 proportional abundances of genera), and with the analogue matching by evaluating whether
220 Anthropocene assemblages extend beyond the variation defined by the Holocene assemblages
221 (using Bray-Curtis distances between the Holocene centroid and individual Anthropocene
222 assemblages, 41-45).

223
224 **(f) Effects of time averaging on regime shifts in simulations.** We investigate the effect of
225 time averaging on the detection of the regime shift over a broad range of values, from 1 year
226 up to 1,000 years in simulations. This range reflects the IQR values observed in the Adriatic
227 Sea: time averaging varies by two orders of magnitude between the Po prodelta with decadal
228 IQR, the Isonzo prodelta with centennial IQR, and sites off Istria with millennial IQR. We
229 simulate the effects of time averaging (1) on the timing and the abruptness of shifts and (2) on
230 the estimate of ω with two scenarios. In a first scenario, we assess the sensitivity of ω in a
231 stasis model with $\theta_1 = 1$ in a Holocene-scale simulation with 10,000 years, varying true ω
232 between 0.01 and 0.2 (values comparable to empirical estimates). In a second scenario,
233 tailored to the past 200 years to capture sedimentation conditions at Po and Isonzo prodeltas,
234 the abrupt increase in size from $\theta_1 = 1$ (2.7 mm) to $\theta_2 = 2$ (7.4 mm) occurs in 1950 and the
235 true ω of non-averaged time series is set to 0.01. In this Anthropocene simulation, we assess
236 what eco-evolutionary size models are best supported as time averaging increases. In both
237 scenarios, we sample 50 individuals in each of the thirty increments (comparable to the
238 number of increments and sample sizes in 1.5 m-long cores), and fit time-averaged time series

239 with the same methods as empirical time series. We repeat simulations 1,000 times, estimate
240 means of ω in Holocene-scale simulations, and compute model-specific Akaike weights in
241 Anthropocene simulations, with 95% confidence intervals.

242

243 **3. Results**

244 *(a) Size shift in the northern Adriatic Sea*

245 The size structure of *C. gibba* in Anthropocene assemblages (figure 1B) does not overlap with
246 TST (10-7 kyr ago) and HST (~7 kyr ago up to the 19th century) assemblages in principal
247 coordinate analysis (figure 1B, table S5-S6), and 50% of Anthropocene assemblages are
248 farther from the Holocene centroid in terms of the Frechet distances than 97.5% of Holocene
249 assemblages (figure 2A). TST and HST increments do not differ in size structure and are both
250 characterized by right-skewed, thin-tailed distributions dominated by individuals < 5 mm
251 (black histograms in figure 1A). Anthropocene assemblages (white histograms in figure 1A)
252 from high-sedimentation sites (>0.2 cm/y) with centennial to decadal IQR at the Po and
253 Isonzo prodeltas are characterized by bimodal distributions with abundant large individuals (>
254 10 mm). Low-sedimentation sites with millennial IQR generated by mixing of Anthropocene
255 and HST assemblages in top-core increments are characterized by heavy-tailed distributions,
256 with individuals > 5 mm being moderately frequent (figure 1A). The shift between the TST
257 and HST assemblages on one hand and Anthropocene assemblages on the other hand is driven
258 by the appearance of individuals > 10 mm. The mean and the 95th percentile log-length of *C.*
259 *gibba* in death assemblages correlate positively with the 1970-2010 measurements of yearly
260 frequency of seasonal hypoxia at 16 sites (Spearman $r = 0.91$, $p = 0.005$) and the 95th
261 percentile log-length (Spearman $r = 0.82$, $p < 0.0001$). The 95th percentile log-length increases
262 abruptly at 10% probability of yearly hypoxia (figure 2B), suggesting that the switch from the
263 right-skewed to bimodal state occurs at low frequency of hypoxia.

264

265 ***(b) Compositional shift in the northern Adriatic Sea***

266 The size shift coincides with a shift in the molluscan composition. The Bray-Curtis distances
267 show that 82% of Anthropocene living assemblages are further from the Holocene centroid
268 than 97.5% of individual Holocene assemblages (figure 2B). The Holocene abundance
269 increases from ~20-30% (95% confidence intervals on the median value) in TST and HST
270 increments to 50-60% in time-averaged death assemblages and to 63-75% in Anthropocene
271 non-averaged living assemblages (figure 2C). The increase in abundance of *C. gibba* is
272 compensated by the decline in abundance of commensals, predators and scavengers (figure
273 S7). Principal coordinate analyses and PERMANOVA show that the overlap between
274 Anthropocene living and death assemblages on one hand and Holocene assemblages on the
275 other hand is negligible (figure 2E, table S5).

276

277 ***(c) Chronological and stratigraphic record of size shifts***

278 Threshold regressions and model fitting show that chronological records in size at Po are best
279 explained by an abrupt punctuational increase in the mean log-length (from $\theta_1 = 1.07$ to $\theta_2 =$
280 1.53 , with $\omega = 0.007$) and in the 95th percentile log-length (from $\theta_1 = 1.6$ to $\theta_2 = 2.3$, with $\omega =$
281 0.022) that occurred within a single decade at ~1950 (figure 3A, 4A). This shift separates
282 populations exhibiting stasis prior to (right-skewed distributions) and after 1950 (bimodal
283 distributions). Stratigraphic records at sites with high sedimentation (> 0.2 cm/y) at Po and
284 Isonzo also support a single abrupt shift both in the mean and the 95th percentile log-length (in
285 the mid-20th century at 80-110 cm at Po and in the late 19th century at 30-35 cm at Isonzo,
286 figure 3B, 4B). These shifts are best explained by the punctuation between two stasis
287 segments or by the shift from stasis to random walk (figure 3B), and thus capture similar
288 dynamics as the chronological records. In contrast, stratigraphic records at sites with slow

289 sedimentation (~ 0.01 cm/y) either detect a size decline between the TST and HST units or do
290 not show any shifts, and estimates of ω are smaller than at Po and Isonzo (figure 4C).
291 Although the signature of the size increase in the 20th century is lost at these sites, TST and
292 HST assemblages are consistently dominated by small-size individuals whereas the top-core
293 mixtures of highstand and Anthropocene shells averaged to millennia are heavy-tailed and
294 thus still detect the signature of the 20th century size increase (figure 1B). These heavy-tailed
295 assemblages become bimodal when old shells without the surficial periostracum layer are
296 excluded (figure S2-S3). Therefore, body size shifts during the Holocene until the 20th century
297 are of smaller magnitude than the size increase observed in the 20th century.

298 Although the Po and Isonzo records with the upcore transition from centennial to
299 decadal averaging in the 20th century deposits capture the abrupt increase in size relatively
300 well, size changes within HST increments at sites with millennial averaging are very muted
301 and support a single stasis model (figure 4A-B). This difference in the stratigraphic
302 expression of size pattern is confirmed by simulations of abrupt size-increase in 1950, which
303 predict that the punctuation is preserved when the magnitude of time averaging does not
304 exceed ~ 20 -50 years (figure 4D-E). The variance (ω) in the mean and in the 95th percentile
305 log-length declines by two orders of magnitude with time averaging increasing from decadal
306 to millennial values, both in the empirical and simulated stratigraphic records (figure 4C, FF).
307 This effect pulls the size trajectory in the stratigraphic record towards stronger stasis and
308 towards very small ω at sites with slow sedimentation. The pull by time averaging is avoided
309 at Po and Isonzo because punctuations at these sites coincide with the upcore decline in time
310 averaging from 30 to ~ 15 years at Po and from 75 to ~ 10 -20 years at Isonzo (figure 2). The
311 stratigraphic records at the Po and Isonzo prodeltas thus distinctly preserve the 20th century
312 shift (under high or moderate sediment accumulation rates) because IQRs of the late 20th
313 century assemblages are low. Under higher depth and rate of bioturbation that characterized

314 these environments prior to 1950s, multi-decadal time averaging strongly mutes the
315 stratigraphic signal in size patterns even under relatively high sedimentation rates (figure 4D-
316 E).

317

318 **4. Discussion**

319 The abrupt increase in size of *C. gibba* detected in the stratigraphic records from the Po and
320 Isonzo prodeltas and the observation that large individuals are invariably rare in the pre-
321 Anthropocene assemblages at sites with slow sedimentation demonstrate that the shift in
322 maximum shell size from 5 to 10-15 mm occurred in the whole northern Adriatic Sea (figures
323 1A, 2A). The comparison of the Holocene with the late 20th century assemblages
324 demonstrates that this change reflects community-wide shift because it was associated with a
325 shift in genus-level molluscan composition (figure 2B), characterized by an increase in the
326 dominance of *C. gibba* (figure 2C). Although *C. gibba* was a persistent subset of molluscan
327 communities during the Holocene (49-50), it became dominant relative to other molluscan
328 species in the 20th century. The bimodality of abundances prior to and after the transition in
329 the 20th century (figure 2C) is a diagnostic attribute of abrupt ecological transitions (51). The
330 intermediate position of Anthropocene death assemblages with *C. gibba* located between
331 Holocene assemblages and Anthropocene living assemblages is probably driven by
332 taphonomic inertia (mixing of Anthropocene shells with older shells of other species).
333 Multiple lines of evidence indicate that the regime shift was determined by high frequency of
334 seasonal hypoxia. First, the increase in size and dominance of *C. gibba* coincided with the late
335 20th century eutrophication that was coupled with an increase in the frequency of hypoxic
336 events (36, 52). Although seasonal hypoxia occasionally affected benthic communities also
337 prior to the 20th century, the recurrence of hypoxic events was less frequent (38). Second,
338 assemblages that remained small-sized in the 20th century were located above the seasonal

339 thermocline at Isonzo prodelta and in the Gulf of Venice, and thus, were not affected by
340 seasonal hypoxia. Third, both size indices increase with the relative frequency of seasonal
341 hypoxia at 16 sites (figure 2B), and the abrupt increase in the 95th percentile log-length
342 indicates that the shift between the two states follows a threshold-type dynamic and can
343 already occur if seasonal hypoxia occurs in one year per decade. *C. gibba* was observed to
344 grow rapidly to > 11 mm over two years in the aftermath of seasonal anoxia (53). Direct
345 biological observations showed that seasonal mass mortalities in the Adriatic Sea negatively
346 affected predators and substrate-destabilizing burrowers, including burrowing shrimps,
347 echinoids, holothurians, predatory asteroids and muricid gastropods (54), in contrast to
348 hypoxia-tolerant *C. gibba* (55-56). The recovery of these taxa in the wake of hypoxic events is
349 delayed and occurs over several years (57), allowing *Corbula* dominance also in years
350 without seasonal hypoxic events. The size and dominance increase following the shift to
351 higher frequency might be hypothesized to be driven by the predatory and competitive release
352 and by high tolerance of *C. gibba* to seasonal hypoxia (58). This release hypothesis is
353 congruent with the decline in abundance of predatory gastropods observed here and with the
354 20th century decline in the depth of the surface mixed layer declined from several decimeters
355 documented at Po and Isonzo prodeltas on the basis of higher preservation of flood layers,
356 reduced mottling, and reduced time averaging (36).

357 Although low sedimentation rates that lead to multi-decadal or millennial time
358 averaging will strongly reduce temporal variance in body size and will bias abrupt shifts
359 towards gradual trends, relatively high sedimentation rates (> 0.2 cm/y) are also not sufficient
360 for the preservation of high-resolution ecological dynamic in the fossil record if associated
361 with bioturbation. However, the temporal association of the size and compositional changes in
362 the molluscan community with the declining bioturbation indicates a common cause behind
363 the regime shift and its preservation potential in the fossil record. We thus posit that the

364 preservation of abrupt regime shifts in the stratigraphic record is triggered by the pervasive
365 ecosystem change of sufficient, decadal-scale duration that is associated with the decline in
366 bioturbational mixing, especially in settings with high to moderate net accumulation rates and
367 without long hiatuses. The Anthropocene regime shifts in the nature of macrobenthic
368 communities in the northern Adriatic Sea are not only unprecedented relative to the Holocene
369 history but are also sufficiently strong and temporally persistent so that they have the potential
370 to be distinctly preserved in the stratigraphic record, paralleling Anthropocene shifts in
371 geochemical and microbiotic proxies documented in marginal marine environments (59-60).
372 We suggest that differences in the intensity of bioturbation between extinction regimes with
373 limited bioturbation and background regimes with intense bioturbation can generate a
374 dichotomy in the resolution of the marine fossil record on continental shelves. On one hand,
375 the majority of the fossil record that formed in shelf ecosystems with intense bioturbation
376 throughout most of the Holocene is probably averaged to centuries or millennia (61) and rich
377 in gaps (62). On the other hand, the window for preservation of highly-resolved ecological
378 dynamic on marine shelves probably opens in the aftermath of anthropogenic regime shifts on
379 the present-day shelves and was probably open in the wake of major ecosystem perturbations
380 in the past (63). The window for preservation is not equivalent to anoxic conditions that
381 simply exclude burrowers but is rather determined by the recovery dynamic of burrowers in
382 the aftermath of disturbances, e.g., by time to habitat recolonization from regions not affected
383 by extinctions, by incumbency and by source-sink effects at ecological scales, or by time to
384 speciation at evolutionary time scales.

385

386

387 **Data access and availability**

388 Original size data will be uploaded to Data Dryad.

389 **Author contributions:**

390 A.T. and M.Z. designed the research, P.G.A., T.F., I.G., A.H., M.K., R.N., V.N. and D.S.
391 collected the data, A.T. compiled and analyzed the data, and all authors discussed the results
392 and contributed to the writing of the manuscript.

393 **Competing interests.** We declare we have no competing interests.

394 **Funding.** This study was funded by the Austrian Science Fund (FWF project P24901), the
395 Slovak Scientific Grant Agency (VEGA 0169-19), Slovak Research and Development
396 Agency (APVV17-0555), and the National Science Foundation (EAR-0920075 and EAR-
397 1559196).

398 **Acknowledgements.** The authors thank S.M. Holland and an anonymous referee for critical
399 comments.

400 **Electronic Supplementary Material** includes details on data, methods, tables and figures.

401

402 **References**

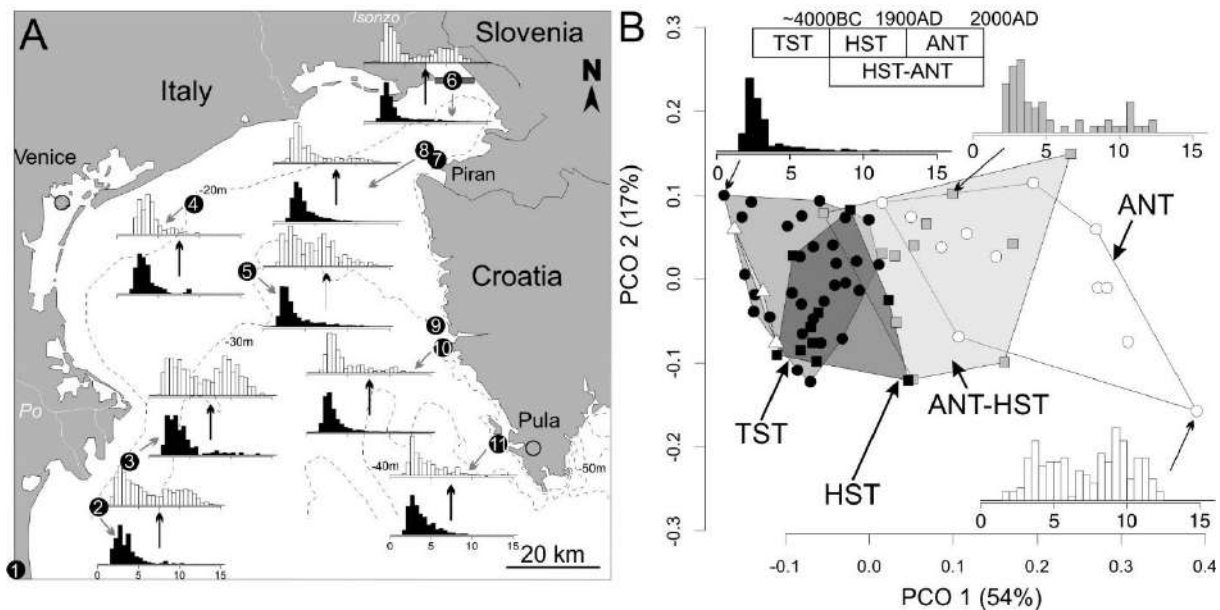
- 403 1. Petersen JK, Hansen JW, Laursen MB, Clausen P, Carstensen J, Conley DJ 2008 Regime
404 shift in a coastal marine ecosystem. *Ecol Appl* **18**, 497-510.
- 405 3. Villnäs A, Norkko A 2011 Benthic diversity gradients and shifting baselines: implications
406 for assessing environmental status. *Ecol Appl* **21**, 2172-2186.
- 407 3. Rombouts I et al 2013 Evaluating marine ecosystem health: case studies of indicators using
408 direct observations and modelling methods. *Ecol Indic* **24**, 353-365.
- 409 4. Di Camillo CG, Cerrano C 2015 Mass mortality events in the NW Adriatic Sea: phase shift
410 from slow-to fast-growing organisms. *PloS one* **10**, e0126689.
- 411 5. Rocha J et al. 2015 A holistic view of marine regime shifts. *Philos T Roy Soc B* **370**,
412 20130273.
- 413 6. Dornelas M, Gotelli NJ, Shimadzu H, Moyes F, Magurran AE, McGill BJ 2019 A balance
414 of winners and losers in the Anthropocene. *Ecol Lett* **22**, 847-854.
- 415 7. Chase JM et al 2019 Species richness change across spatial scales. *Oikos* **128**, 1079-1091.
- 416 8. Aronson RB, Macintyre IG, Wapnick CM, O'Neill MW 2004 Phase shifts, alternative
417 states, and the unprecedented convergence of two reef systems. *Ecology* **85**, 1876-1891.

- 418 9. Pandolfi JM and Jackson, J.B., 2006. Ecological persistence interrupted in Caribbean coral
419 reefs. *Ecology Letters* **9**, 818-826.
- 420 10. Kidwell SM 2007. Discordance between living and death assemblages as evidence for
421 anthropogenic ecological change. *Proc Natl Acad Sci USA* **104**, 17701-17706.
- 422 11. Williams JW, Blois JL, Shuman BN 2011 Extrinsic and intrinsic forcing of abrupt
423 ecological change: case studies from the late Quaternary. *J Ecol* **99**, 664-677.1.
- 424 12. Tomašových, A. and Kidwell, S.M., 2017. Nineteenth-century collapse of a benthic
425 marine ecosystem on the open continental shelf. *Proc Biol Sci* **284**, 20170328.
- 426 13. Keller G et al. 2018 Environmental changes during the cretaceous-Paleogene mass
427 extinction and Paleocene-Eocene thermal maximum: implications for the
428 Anthropocene. *Gondwana Res* **56**, 69-89.
- 429 14. Aberhan M, Kiessling W 2015 Persistent ecological shifts in marine molluscan
430 assemblages across the end-Cretaceous mass extinction. *Proc Natl Acad Sci USA* **112**, 7207-
431 7212.
- 432 15. Penn JL et al. 2018 Temperature-dependent hypoxia explains biogeography and severity
433 of end-Permian marine mass extinction. *Science* **362**, eaat1327.
- 434 16. Kidwell SM, Tomasovych A 2013 Implications of time-averaged death assemblages for
435 ecology and conservation biology. *Annu Rev Ecol Evol S* **44**, 539-563.
- 436 17. Kosnik MA et al. 2017 Sediment mixing and stratigraphic disorder revealed by the age-
437 structure of *Tellina* shells in Great Barrier Reef sediment. *Geology* **35**, 811-814.
- 438 18. Rabalais NN et al. 2007 Sediments tell the history of eutrophication and hypoxia in the
439 northern Gulf of Mexico. *Ecol Appl* **17**, S129-S143.
- 440 19. Willis KJ et al. 2010 Biodiversity baselines, thresholds and resilience: testing predictions
441 and assumptions using palaeoecological data. *Trends Ecol Evol* **25**, 583-591.
- 442 20. Jonkers L et al. 2013 Global change drives modern plankton communities away from the
443 pre-industrial state. *Nature* **570**, 372-375.
- 444 21. Leonard-Pingel JS et al. 2019 Gauging benthic recovery from 20th century pollution on
445 the southern California continental shelf using bivalves from sediment cores. *Mar Ecol Prog*
446 *Ser* **615**, 101-119.
- 447 22. Tomašových A, Kidwell SM, Alexander CR, Kaufman DS 2019 Millennial-scale age
448 offsets within fossil assemblages: result of bioturbation below the taphonomic active zone and
449 out-of-phase production. *Paleoceanogr Paleocl* **34**, 954-977.
- 450 21. Sadler PM 1981 Sediment accumulation rates and the completeness of stratigraphic
451 sections. *J Geol* **89**, 569-584.

- 452 22. Tomašových A, Kidwell SM 2010 The effects of temporal resolution on species turnover
453 and on testing metacommunity models. *Am Nat* **175**, 587-606.
- 454 23. Kemp DB et al. 2015 Maximum rates of climate change are systematically underestimated
455 in the geological record. *Nature Comm* **6**, 8890.
- 456 24. Holland SM 2016 The non-uniformity of fossil preservation. *Philos T Roy Soc B* **371**,
457 20150130.
- 458 25. Löwemark L, Grootes PM 2004 Large age differences between planktic foraminifers
459 caused by abundance variations and *Zoophycos* bioturbation. *Paleoceanography* **19**, PA2001.
- 460 26. Steiner Z, Lazar B, Levi S, Tsroya S, Pelled O, Bookman R, Erez J 2016 The effect of
461 bioturbation in pelagic sediments: lessons from radioactive tracers and planktonic
462 foraminifera in the Gulf of Aqaba, Red Sea. *Geochim Cosmochim Ac* **194**, 139-152.
- 463 27. Twitchett RJ 2007 The Lilliput effect in the aftermath of the end-Permian extinction
464 event. *Palaeogeogr Palaeoclimatol Palaeoecol* **252**, 132-144.
- 465 28. Levin LA, Ekau W, Gooday AJ, Jorissen F, Middelburg JJ, Naqvi SWA, Neira C,
466 Rabalais NN, Zhang J 2009 Effects of natural and human-induced hypoxia on coastal benthos,
467 *Biogeosciences* **6**, 2063–2098,
- 468 29. Rick TC, Reeder-Myers LA, Hofman CA, Breitburg D, Lockwood R, Henkes G, Kellogg
469 L, Lowery D, Luckenbach MW, Mann R, Ogburn MB 2016 Millennial-scale sustainability of
470 the Chesapeake Bay Native American oyster fishery. *Proc Natl Acad Sci USA* **113**, 6568-
471 6573.
- 472 30. Payne JL et al. 2016 Ecological selectivity of the emerging mass extinction in the oceans.
473 *Science* **353**, 1284-1286.
- 474 31. Dornelas M et al. 2013 Quantifying temporal change in biodiversity: challenges and
475 opportunities. *Proc Biol Sci* **280**, 20121931.
- 476 32. Hunt G. 2012 Measuring rates of phenotypic evolution and the inseparability of tempo
477 and mode measuring rates of phenotypic evolution. *Paleobiology* **38**, 351-373.
- 478 33. Amorosi A, et al 2003 Facies architecture and latest Pleistocene–Holocene depositional
479 history of the Po Delta (Comacchio area), Italy. *J Geol* **111**, 39-56.
- 480 34. Scarponi D, Kaufman D, Amorosi A, Kowalewski M 2013 Sequence stratigraphy and the
481 resolution of the fossil record. *Geology* **41**, 239-242.
- 482 35. Albano PG, Gallmetzer I, Haselmair A, Tomašových A, Stachowitsch M, Zuschin M,
483 2018 Historical ecology of a biological invasion: the interplay of eutrophication and pollution
484 determines time lags in establishment and detection. *Biological Invasions* **20**, 1417-1430

- 485 36. Tomašových A et al. 2018 Tracing the effects of eutrophication on molluscan
486 communities in sediment cores: outbreaks of an opportunistic species coincide with reduced
487 bioturbation and high frequency of hypoxia in the Adriatic Sea. *Paleobiology* **44**, 575-602.
- 488 37. Tomašových A, et al. 2019 A decline in molluscan carbonate production driven by the
489 loss of vegetated habitats encoded in the Holocene sedimentary record of the Gulf of
490 Trieste. *Sedimentology* **66**, 781-807.
- 491 38. Tomašových A et al. 2017 Stratigraphic unmixing reveals repeated hypoxia events over
492 the past 500 yr in the northern Adriatic Sea. *Geology* **45**, 363-366.
- 493 39. Schnedl SM, et al. 2018 Molluscan benthic communities at Brijuni Islands (northern
494 Adriatic Sea) shaped by Holocene sea-level rise and recent human eutrophication and
495 pollution. *Holocene* **28**, 1801-1817.
- 496 40. Gallmetzer I, et al. 2019 Tracing origin and collapse of Holocene benthic baseline
497 communities in the northern Adriatic. *Palaios* **34**, 121-145.
- 498 41. Gavin DG, Oswald WW, Wahl ER, Williams JW 2003 A statistical approach to
499 evaluating distance metrics and analog assignments for pollen records. *Quaternary Res* **60**,
500 356-367.
- 501 42. Simpson, GL 2007 Analogue methods in palaeoecology: using the analogue package. *J*
502 *Stat Softw* **22**, 1-29.
- 503 43. Goberville E, Beaugrand G, Sautour B, Tréguer P 2011 Evaluation of coastal
504 perturbations: a new mathematical procedure to detect changes in the reference state of
505 coastal systems. *Ecol Indic* **11**, 1290-1300.
- 506 44. Tomašových A, Kidwell SM 2011 Accounting for the effects of biological variability and
507 temporal autocorrelation in assessing the preservation of species abundance. *Paleobiology* **37**,
508 332-354.
- 509 45. Anderson MJ, Walsh DC 2013 PERMANOVA, ANOSIM, and the Mantel test in the face
510 of heterogeneous dispersions: what null hypothesis are you testing? *Ecol Monogr* **83**, 557-
511 574.
- 512 46. Hunt G 2008 Gradual or pulsed evolution: when should punctuational explanations be
513 preferred? *Paleobiology* **34**, 360-377.
- 514 47. Hunt G, Hopkins MJ, Lidgard, S 2015 Simple versus complex models of trait evolution
515 and stasis as a response to environmental change. *Proc Natl Acad Sci USA* **112**, 4885-4890.
- 516 48. Sheets HD, Mitchell CE 2001 Why the null matters: statistical tests, random walks and
517 evolution. In *Microevolution Rate, Pattern, Process* (pp. 105-125). Springer, Dordrecht.

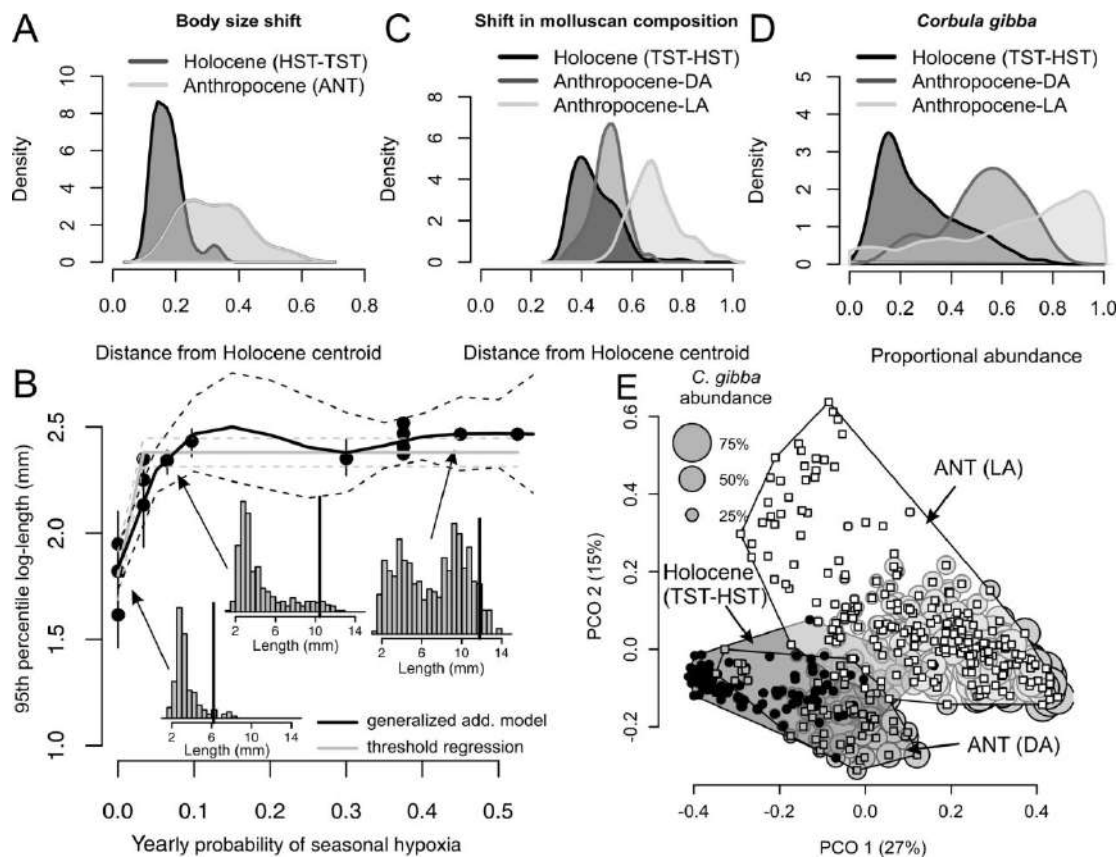
- 518 49. Scarponi D, Kowalewski M 2007 Sequence stratigraphic anatomy of diversity patterns:
519 Late Quaternary benthic mollusks of the Po Plain, Italy. *Palaios* **22**, 296-305.
- 520 50. Kowalewski M, Wittmer JM, Dexter TA, Amorosi A, Scarponi D 2015 Differential
521 responses of marine communities to natural and anthropogenic changes. *Proc Biol Sci* **282**,
522 20142990.
- 523 51. Bestelmeyer BT et al 2011 Analysis of abrupt transitions in ecological
524 systems. *Ecosphere* **2**, 1-26.
- 525 52. Justić D 1991 Hypoxic conditions in the northern Adriatic Sea: historical development
526 and ecological significance. *Geol Soc Spec Publ* **58**, 95-105.
- 527 53. Hrs-Brenko M 2003 The role of bivalve *Corbula gibba* (Olivi, 1792) (Corbulidae,
528 Mollusca Bivalvia) in the recruitment of benthic communities in the northern
529 Adriatic. *Pomorski Zbornik* **41**, 195–208.
- 530 54. Stachowitsch M 1984 Mass mortality in the Gulf of Trieste: the course of community
531 destruction. *Mar Ecol* **5**, 243-264.
- 532 55. Holmes SP, Miller N 2006, Aspects of the ecology and population genetics of the bivalve
533 *Corbula gibba*. *Mar Ecol Prog Ser* **315**, 129-140.
- 534 56. Stachowitsch M 1991 Anoxia in the Northern Adriatic Sea: rapid death, slow recovery.
535 *Geol Soc Spec Publ* **58**, 119-129.
- 536 57. Riedel B, Pados T, Pretterebner K, Schiemer L, Steckbauer A, Haselmair A, Zuschin M,
537 Stachowitsch M 2014 Effect of hypoxia and anoxia on invertebrate behaviour: ecological
538 perspectives from species to community level. *Biogeosciences* **11**, 1491-1518.
- 539 58. Yoder JB et al 2010 Ecological opportunity and the origin of adaptive radiations. *J Evol*
540 *Biol* **23**, 1581-1596.
- 541 59. Waters CN et al 2016 The Anthropocene is functionally and stratigraphically distinct from
542 the Holocene. *Science* **351**, aad2622.
- 543 60. Wilkinson IP et al. 2014 Microbiotic signatures of the Anthropocene in marginal marine
544 and freshwater palaeoenvironments. *Geol Soc Spec Publ* **395**, 185-219.
- 545 61. Kidwell SM 2013 Time-averaging and fidelity of modern death assemblages: building a
546 taphonomic foundation for conservation palaeobiology. *Palaeontology* **56**, 487-522.
- 547 62. Holland SM, Patzkowsky ME 2015 The stratigraphy of mass extinction. *Palaeontology*
548 **58**, 903-924.
- 549 63. Hofmann RL et al 2015 Loss of the sedimentary mixed layer as a result of the end-
550 Permian extinction. *Palaeogeogr Palaeoclimatol Palaeoecol* **428**, 1-11

552 **Figure Legends**

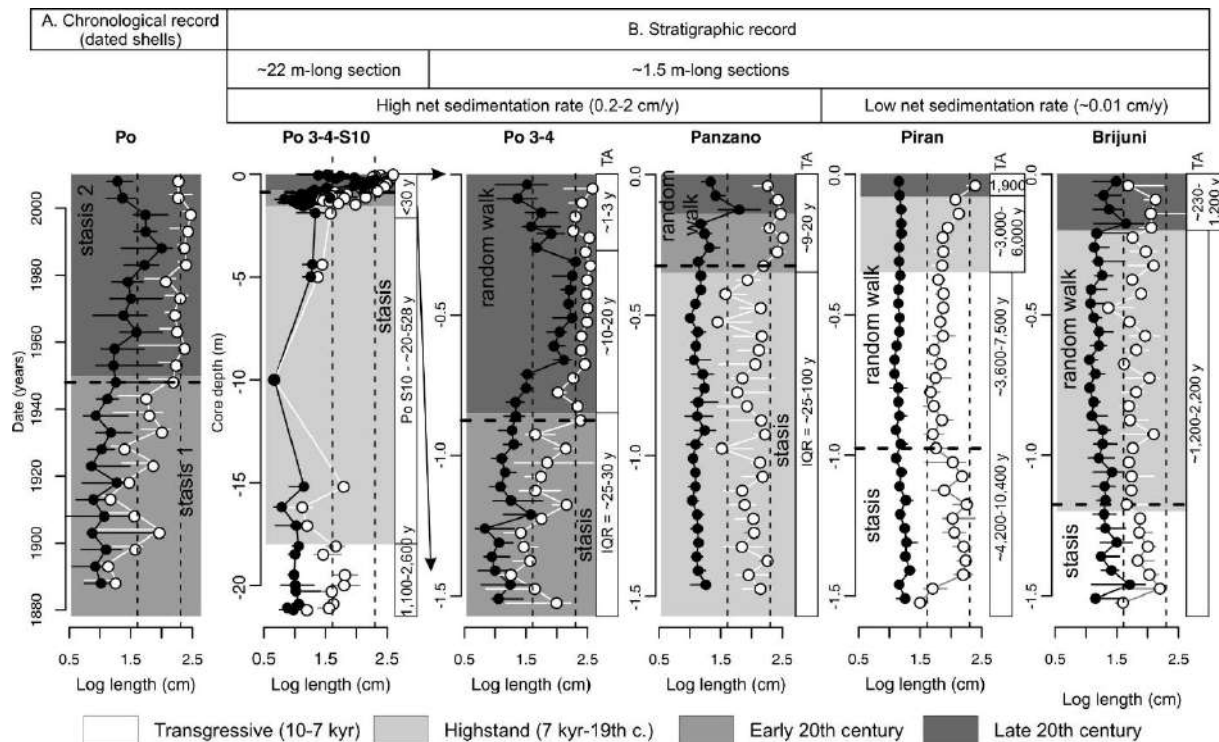
553
 554 **Figure 1.** Size distributions of *C. gibba* in Holocene (TST and HST) and Anthropocene (20th
 555 century) death assemblages in the northern Adriatic Sea (with the exception of three
 556 Anthropocene sites from < 10 m depth, all sites are > 10 m deep). A. Holocene-Anthropocene
 557 site pairs based on eight sites show that right-skewed and thin-tailed HST assemblages (black)
 558 are replaced by bimodal (under low time averaging) or heavy-tailed (under high averaging)
 559 Anthropocene assemblages (white). The labels summarize all stations analyzed in this study:
 560 1 – Po Plain core S10, 2 – Po 4, 3 – Po 3, 4 – Venice, 5 – Station D in the Gulf of Venice, 6 –
 561 Bay of Panzano transect, 7 – Piran 1, 8 – Piran 2, 9-10 – Rovinj 120 and 38, 11 – Brijuni. The
 562 shift at sites with high time averaging (sites 5 and 10) is based on shells with (white) and
 563 without (black) periostracum. B. The size structure of *C. gibba* differs between Holocene
 564 (TST and HST) and Anthropocene (ANT) assemblages (at sites > 10 m water depth, white
 565 circles) in principal coordinate analysis based on 10-30 cm-thick increments. The highstand-
 566 Anthropocene (ANT-HST) assemblages at sites with high time averaging (> 10 m water
 567 depth) are based on shells with periostracum (gray squares). Three Anthropocene assemblages
 568 at < 10 m water depth are represented by white triangles.

569

570



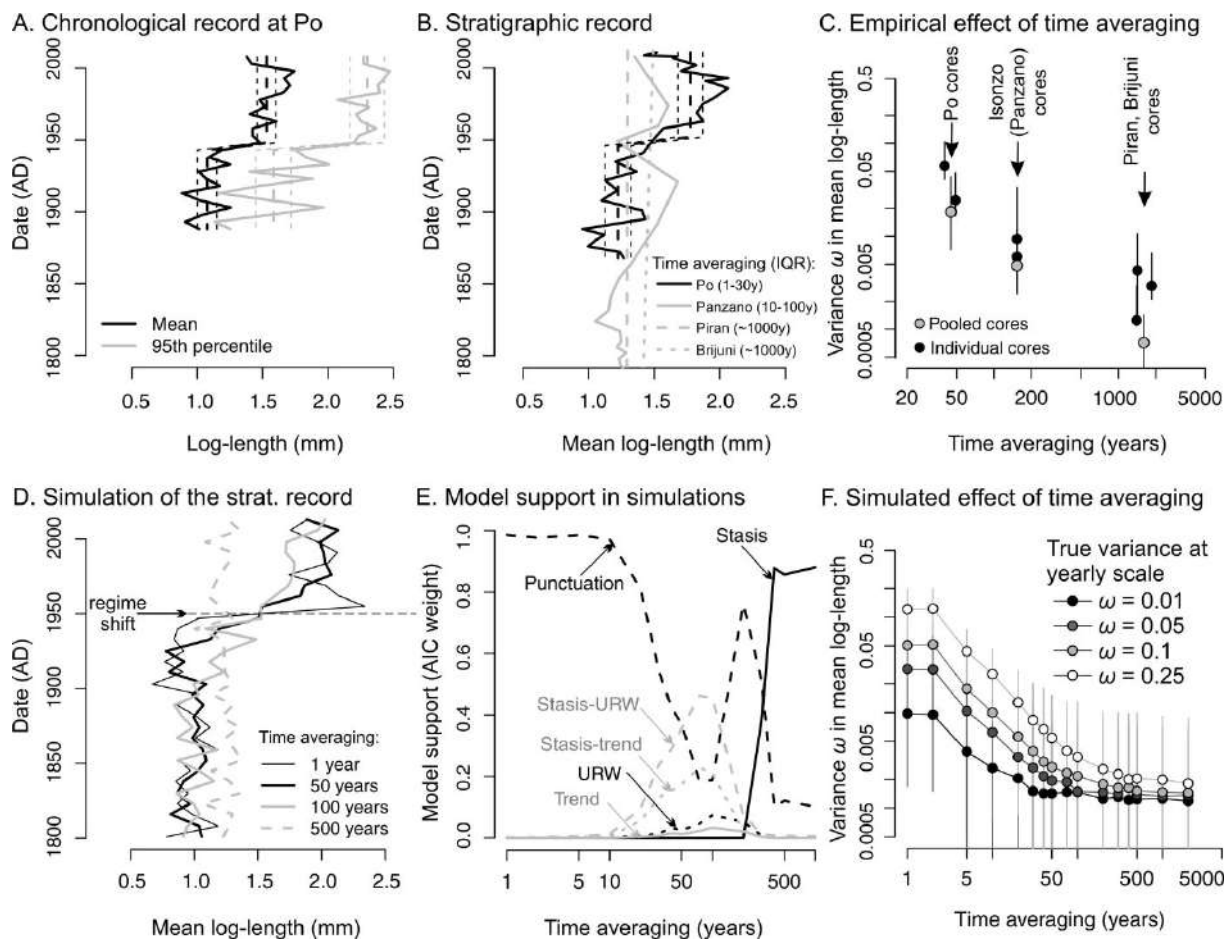
571
 572 **Figure 2.** The size and compositional regime shift between Holocene and Anthropocene
 573 assemblages and the effect of oxygen concentrations on shell size of *C. gibba*. A. Overlap in
 574 size structure between Holocene and Anthropocene assemblages: density kernels show that
 575 the Frechet distances from the Holocene centroid to Anthropocene assemblages (light gray)
 576 exceed those between Holocene assemblages and the Holocene centroid (dark gray). B. The
 577 nonlinear increase in the 95th percentile log-length of *C. gibba* in death assemblages (based on
 578 specimens with periostracum only) to the yearly frequency of seasonal hypoxia (based on data
 579 measured in 1970-2010) can occur if a seasonal hypoxic event occurs at least once during ten
 580 years. C. Compositional overlap between Holocene and Anthropocene assemblages: density
 581 kernels show that the Bray-Curtis distances from the Holocene centroid to Anthropocene
 582 (ANT) living assemblages (LA, light gray) are larger than those among the Holocene
 583 assemblages (dim gray). Anthropocene death assemblages (DA, dark gray) have intermediate
 584 position. D. The bimodal distribution of *C. gibba* abundance, with <20% in HST assemblages,
 585 60% in Anthropocene death assemblages, >80% in living assemblages. E. Genus-level
 586 compositional separation between Holocene (TST and HST), Anthropocene death
 587 assemblages, and Anthropocene living assemblages in principal coordinate analysis. The size
 588 of the bubble plots is scaled to abundance of *C. gibba*.
 589



590

591

592 **Figure 3.** Chronological and stratigraphic records in the mean (black points) and the 95th
 593 percentile log-length (white points) of *Corbula gibba* and the corresponding likelihood
 594 models for temporal changes in the 95th percentile log-length. The punctuational shift in shell
 595 size in the chronological record either translates to stratigraphic punctuation at sites with
 596 relatively high sedimentation (at Po and Isonzo with reduced bioturbation) or to strongly
 597 muted stratigraphic records at sites with very slow sedimentation (at Piran and Brijuni). The
 598 chronological record is based on dated shells partitioned into 5-year cohorts at Po (A). The
 599 stratigraphic records are based on 5-10 cm-thick increments at five sites (B). The 1.5 m-long
 600 core capturing the last ~150 years (Po 3 and Po 4) is shown separately and together with the
 601 S10 core, which extends the record to the onset of the Holocene transgression. Thin vertical
 602 dashed lines demarcate the length at 5 and 10 mm. Error bars refer to 95% bootstrapped
 603 confidence intervals. Time averaging (TA) refers to the interquartile age range in years.



604

605

606

607

608

609

610

611

612

613

614

615

616

617

618

Figure 4. The sensitivity of size shifts to empirical and simulated time averaging. A. The chronological record demonstrates a punctuation in the mean and 95th percentile log-length at Po in the middle of the 20th century. B. The stratigraphic records in the mean log-length at four sites differing in time averaging (IQR in brackets). The black dashed line in A-B is the fit for the Po prodelta based on the threshold regression. C. The negative relationship between time averaging and the variance in mean log-length (ω) observed in the HST increments. ω (with 95% confidence intervals) was estimated at seven sites (two cores at Po, Isonzo, Piran, and one core at Brijuni) and in three pooled cores (Po, Isonzo, Piran). D. Stratigraphic records of the regime shift in the mean log-length occurring in 1950 AD simulated with four levels of time averaging. The thin solid black line refers to one example of non-averaged trajectory (1 year) and the thick solid black lines refer to time-averaged trajectories. E. Based on D, the punctuation is supported at decadal averaging, random-walks and directional trends at 50-200 years, and stasis at > 200 years. F. The negative relationship between time averaging and ω predicted in Holocene-scale simulations.

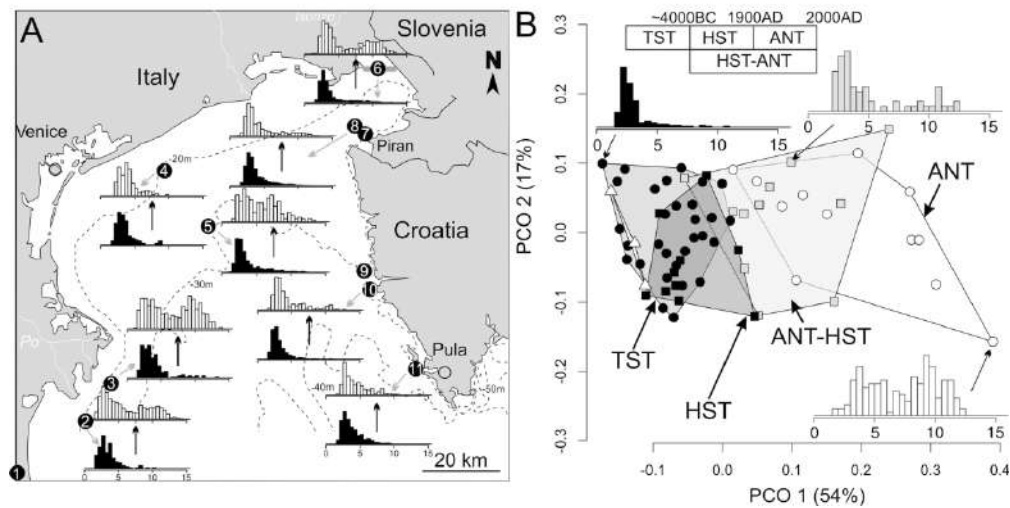


Figure 1. Size distributions of *C. gibba* in Holocene (TST and HST) and Anthropocene (20th century) death assemblages in the northern Adriatic Sea (with the exception of three Anthropocene sites from < 10 m depth, all sites are > 10 m deep). A. Holocene-Anthropocene site pairs based on eight sites show that right-skewed and thin-tailed HST assemblages (black) are replaced by bimodal (under low time averaging) or heavy-tailed (under high averaging) Anthropocene assemblages (white). The labels summarize all stations analyzed in this study: 1 – Po Plain core S10, 2 – Po 4, 3 – Po 3, 4 – Venice, 5 – Station D in the Gulf of Venice, 6 – Bay of Panzano transect, 7 – Piran 1, 8 – Piran 2, 9-10 – Rovinj 120 and 38, 11 – Brijuni. The shift at sites with high time averaging (sites 5 and 10) is based on shells with (white) and without (black) periostracum. B. The size structure of *C. gibba* differs between Holocene (TST and HST) and Anthropocene (ANT) assemblages (at sites > 10 m water depth, white circles) in principal coordinate analysis based on 10-30 cm-thick increments. The highstand-Anthropocene (ANT-HST) assemblages at sites with high time averaging (> 10 m water depth) are based on shells with periostracum (gray squares). Three Anthropocene assemblages at < 10 m water depth are represented by white triangles.

180x97mm (300 x 300 DPI)

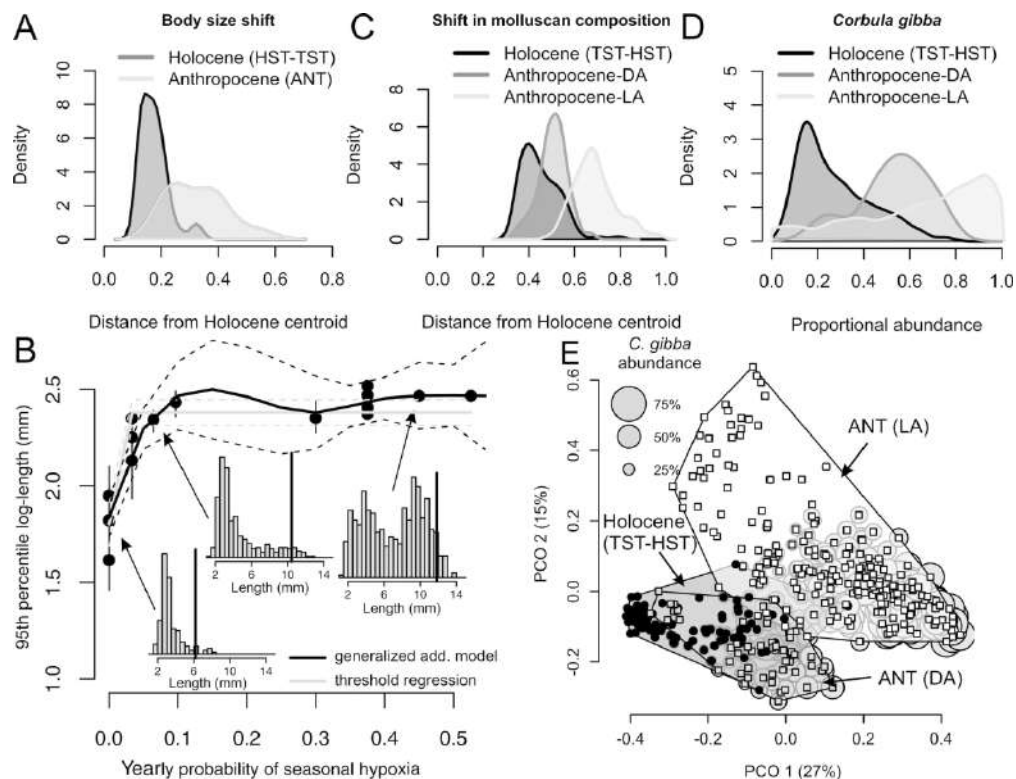


Figure 2. The size and compositional regime shift between Holocene and Anthropocene assemblages and the effect of oxygen concentrations on shell size of *C. gibba*. A. Overlap in size structure between Holocene and Anthropocene assemblages: density kernels show that the Fréchet distances from the Holocene centroid to Anthropocene assemblages (light gray) exceed those between Holocene assemblages and the Holocene centroid (dark gray). B. The nonlinear increase in the 95th percentile log-length of *C. gibba* in death assemblages (based on specimens with periostracum only) to the yearly frequency of seasonal hypoxia (based on data measured in 1970-2010) can occur if a seasonal hypoxic event occurs at least once during ten years. C. Compositional overlap between Holocene and Anthropocene assemblages: density kernels show that the Bray-Curtis distances from the Holocene centroid to Anthropocene (ANT) living assemblages (LA, light gray) are larger than those among the Holocene assemblages (dim gray). Anthropocene death assemblages (DA, dark gray) have intermediate position. D. The bimodal distribution of *C. gibba* abundance, with <20% in HST assemblages, 60% in Anthropocene death assemblages, >80% in living assemblages. E. Genus-level compositional separation between Holocene (TST and HST), Anthropocene death assemblages, and Anthropocene living assemblages in principal coordinate analysis. The size of the bubble plots is scaled to abundance of *C. gibba*.

179x137mm (300 x 300 DPI)

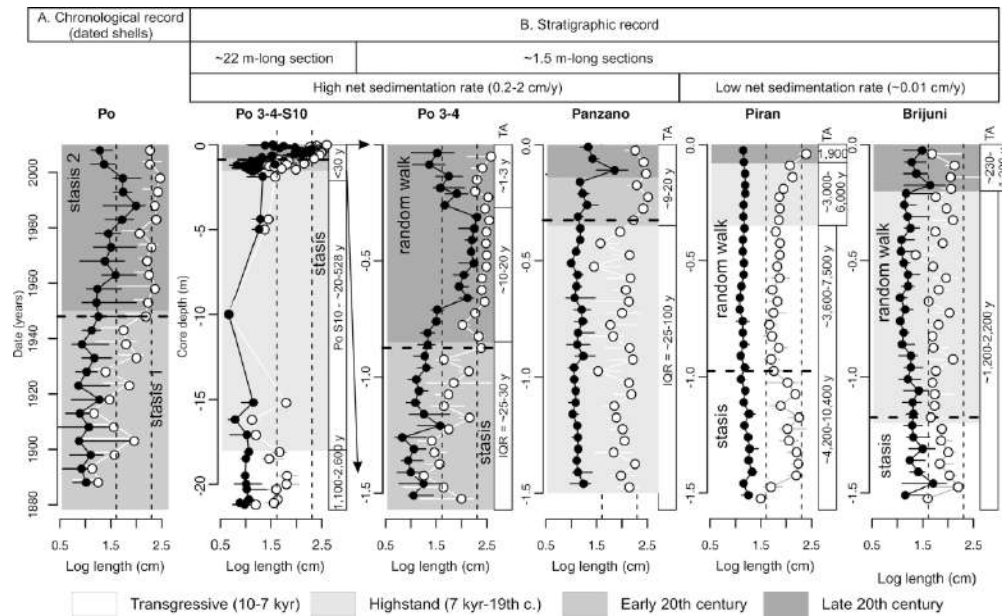


Figure 3. Chronological and stratigraphic records in the mean (black points) and 95th percentile log-length (white points) of *Corbula gibba* and the corresponding likelihood models for temporal changes in the 95th percentile log-length. The punctuational shift in shell size in the chronological record either translates to stratigraphic punctuation at sites with relatively high sedimentation (at Po and Panzano with reduced bioturbation) or to strongly muted stratigraphic records at sites with very slow sedimentation (at Piran and Brijuni). The chronological record is based on dated shells partitioned into 5-year cohorts at Po (A). The stratigraphic records are based on 5-10 cm-thick increments at five sites (B). The 1.5 m-long core capturing the last ~150 years (Po 3 and Po 4) is shown separately and together with the S10 core, which extends the record to the onset of the Holocene transgression. Thin vertical dashed lines demarcate the length at 5 and 10 mm. Error bars refer to 95% bootstrapped confidence intervals. Time averaging (TA) refers to the interquartile age range in years.

201x122mm (300 x 300 DPI)

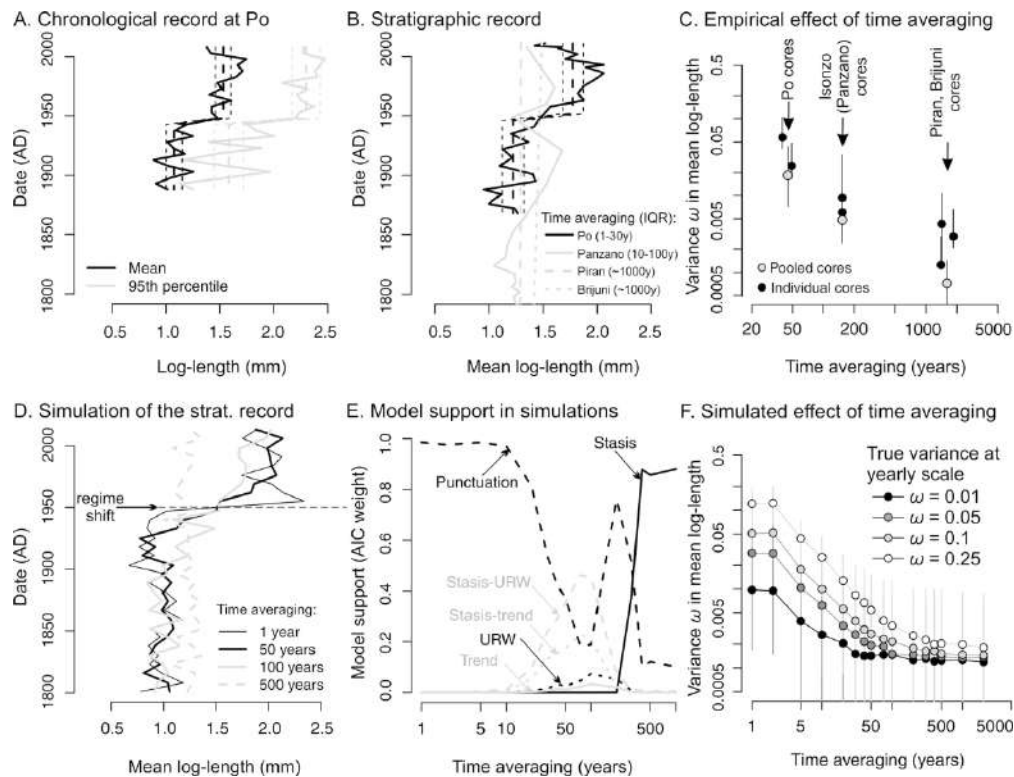


Figure 4. The sensitivity of size shifts to empirical and simulated time averaging. A. The chronological record demonstrates a punctuation in the mean and 95th percentile log-length at Po in the middle of the 20th century. B. The stratigraphic records in the mean log-length at four sites differing in time averaging (IQR in brackets). The black dashed line in A-B is the fit for the Po prodelta based on the threshold regression. C. The negative relationship between time averaging and the variance in mean log-length (ω) observed in the HST increments. ω (with 95% confidence intervals) was estimated at seven sites (two cores at Po, Isonzo, Piran, and one core at Brijuni) and in three pooled cores (Po, Isonzo, Piran). D. Stratigraphic records of the regime shift in the mean log-length occurring in 1950 AD simulated with four levels of time averaging. The thin solid black line refers to one example of non-averaged trajectory (1 year) and the thick solid black lines refer to time-averaged trajectories. E. Based on D, the punctuation is supported at decadal averaging, random-walks and directional trends at 50–200 years, and stasis at > 200 years. F. The negative relationship between time averaging and ω predicted in Holocene-scale simulations.

179x137mm (300 x 300 DPI)